

Interpretation of the Phonon Frequency Shifts in ZnO Quantum Dots

Khan A. Alim, Vladimir A. Fonoberov, and Alexander A. Balandin

Nano-Device Laboratory

Department of Electrical Engineering

University of California – Riverside

Riverside, California 92521

Web-site: <http://ndl.ee.ucr.edu/>

ABSTRACT

Nanostructures made of zinc oxide (ZnO), a wide-bandgap semiconductor, have recently attracted attention due to their proposed applications in low-voltage and short-wavelength (368 nm) electro-optical devices, transparent ultraviolet (UV) protection films, gas sensors, and varistors. Raman spectroscopy presents a powerful tool for identifying specific materials in complex structures and for extracting useful information on properties of nanoscale objects. At the same time the origin of Raman peak deviation from the bulk values is not always well understood for new material systems. There are three main mechanisms that can induce phonon shifts in the free-standing undoped ZnO nanostructures: (i) phonon confinement by the quantum dot boundaries; (ii) phonon localization on defects and (iii) the laser-induced heating in nanostructure ensembles. Here, we report results of the combined non-resonant and resonant Raman scattering studies of an ensemble of ZnO quantum dots with diameter 20 nm. Based on our experimental data, we have been able to identify the origin of the observed phonon frequency shifts. It has been found that the ultraviolet laser heating of the ensemble induces a large red shift of the phonon frequencies. It is calculated that the observed red shift of 14 cm^{-1} corresponds to the local temperature of the quantum dot ensemble of about 700°C .

INTRODUCTION

Zinc oxide (ZnO) presents interesting material system because of its wide band gap of 3.37 eV and some intriguing optical properties. A prominent feature of ZnO is its large exciton binding energy ($\sim 60\text{ meV}$) at room temperature, which results in extreme stability of excitons [1-2]. Raman spectroscopy is a non-destructive characterization method of choice for many recent studies of vibrational properties of ZnO nanostructures. The origin of the frequency shift in ZnO nanostructures is still under debate [3]. In this paper, we present details of the experimental study, which indicates that the large red shift (up to 14 cm^{-1}) in nanocrystals with the diameter of 20 nm is related to local heating rather than to phonon confinement. The experimental results are in excellent agreement with the theory of the optical phonons in wurtzite nanocrystals developed by Fonoberov and Balandin [4-6].

EXPERIMENTAL DETAILS

The samples used for the study are 20 nm powder type ZnO QDs and bulk ZnO sample. The bulk ZnO crystal has wurtzite structure and dimensions $5 \times 5 \times 0.5 \text{ mm}^3$ with the a -plane ($11\bar{2}0$) facet. The investigated ZnO QDs have been produced by the wet chemistry method. The chemical purity of the nanocrystal sample is 99.5%. A Renishaw micro-Raman spectrometer RM 2000 with visible (488 nm) and UV (325 nm) excitation lasers was employed to measure the non-resonant and resonant Raman spectra, correspondingly.

TABLE I. Frequencies (in cm^{-1}) of Raman active phonon modes in bulk ZnO. Presented data is a compilation of the results of different studies listed in Ref. 7.

$E_2(\text{low})$	$A_1(\text{TO})$	$E_1(\text{TO})$	$E_2(\text{high})$	$A_1(\text{LO})$	$E_1(\text{LO})$
102	379	410	439	574	591

RESULTS AND DISCUSSION

The obtained non-resonant Raman spectra of bulk ZnO crystal and ZnO QD sample are shown in Fig. 1. A compilation of the reported frequencies of Raman active phonon modes in bulk ZnO [7-8] is presented in Table I. In the bulk spectrum from Fig. 1, the peak at 439 cm^{-1} corresponds to E_2 (high) phonon, the peak at 410 cm^{-1} corresponds to $E_1(\text{LO})$ and the peak at 379 cm^{-1} corresponds to $A_1(\text{TO})$ phonons. In the QD spectrum, the LO phonon peak at 582 cm^{-1} has a frequency between those of $A_1(\text{LO})$ and $E_1(\text{LO})$ phonons, which is in agreement with theoretical calculations. The broad peak at about 330 cm^{-1} seen in both spectra in Fig. 1 is attributed to the second-order Raman processes.

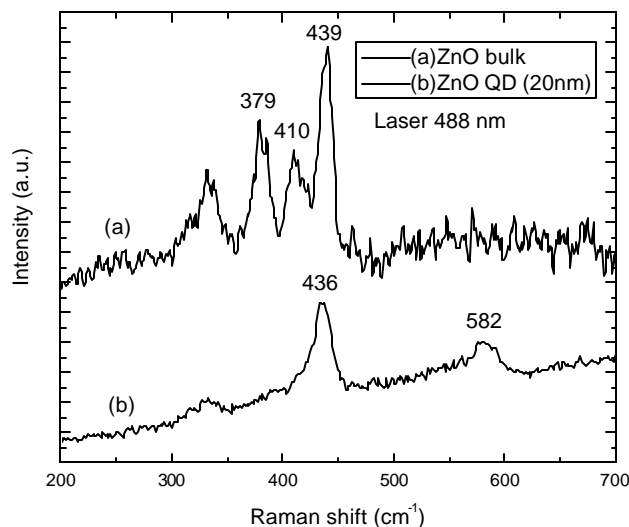


FIG. 1. Non-resonant Raman spectra of (a) ZnO bulk (a-plane) (b) ZnO QD (20nm). Photoluminescence background is subtracted from ZnO bulk spectrum.

In Fig. 1, the E_2 (high) peak in the spectrum of ZnO QDs is redshifted by 3 cm^{-1} from its bulk position. Since the QD size is large, such prominent redshift of the E_2 (high) phonon peak can hardly be explained by the optical phonon confinement. Using the relationship between the temperature T and the relative intensity of Stokes and anti-Stokes peaks $I_S/I_{AS} \approx \exp[\hbar\omega/k_B T]$, we have estimated the local temperature of the ZnO QD powder under visible laser excitation to be 322.73 K ($\sim 50^\circ \text{C}$). Thus, the local heating in the non-resonant Raman spectra cannot be responsible for the observed frequency shift. Therefore, we conclude that the red shift of E_2 (high) phonon peak is due to the presence of intrinsic defects in the ZnO QD samples.

The obtained resonant Raman scattering spectra of bulk ZnO and ZnO QDs, are shown in Fig. 2. Comparing with Table I, 574 cm^{-1} peak corresponds to $A_1(\text{LO})$ phonon in bulk ZnO, other peaks are higher order peaks of LO. $A_1(\text{LO})$ phonon can be observed only when the c -axis is parallel to sample face. When the c -axis is perpendicular to the sample face, the $E_1(\text{LO})$ phonon is observed. Since the size of ZnO QDs is relatively large, the 1LO phonon frequency in QD spectrum should be between 574 cm^{-1} and 591 cm^{-1} . But in the QD spectrum, the 1LO peak appears at 564 cm^{-1} , redshifted by 10 cm^{-1} . The observed huge redshift could hardly be explained by the intrinsic impurities or the quantum confinement effect. We claim here that the huge redshift in the ZnO QDs spectrum is due to intense local heating induced by the laser power. To check this assumption, we varied the UV laser power as well as the area of the illuminated spot on the ZnO QD powder sample and recorded 1LO peak position.

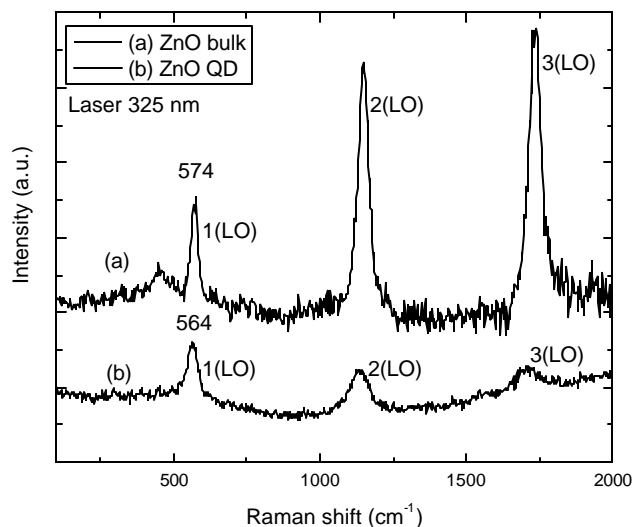


FIG. 2. Resonant Raman spectra of (a) ZnO bulk and (b) ZnO QD. Laser power for ZnO bulk is 20 mW and ZnO QD is 5 mW. Photoluminescence background is subtracted from ZnO bulk spectrum.

The recorded 1LO peak positions under different laser powers and different illuminated spots are shown in Fig. 3 and Fig. 4. It is seen from Fig. 3, that for the illuminated $11 \mu\text{m}^2$ area, the redshift of the LO peak increases almost linearly with UV laser power and reaches about 7 cm^{-1} for the excitation laser power of 20 mW. From Fig. 4, we see the LO peak redshifts at faster rate and reaches about 14 cm^{-1} for $1.6 \mu\text{m}^2$ illuminated spot when the laser power is only 10 mW. In this case, the attempts to record

the LO phonon frequency using UV laser power of 20 mW, resulted in destruction of ZnO nanocrystals in the illuminated spot. The destruction or significant change in the morphology of QDs was confirmed by the absence of any ZnO QDs peak from the same spot at any laser power once the 20 mW power had been used.

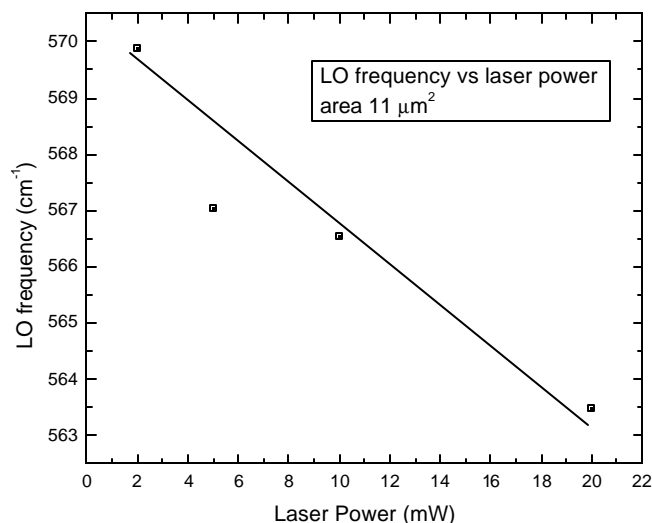


FIG. 3. LO Phonon frequency shift in ZnO quantum dots as a function of laser power. Laser wavelength is 325 nm and laser spot area is $11 \mu\text{m}^2$.

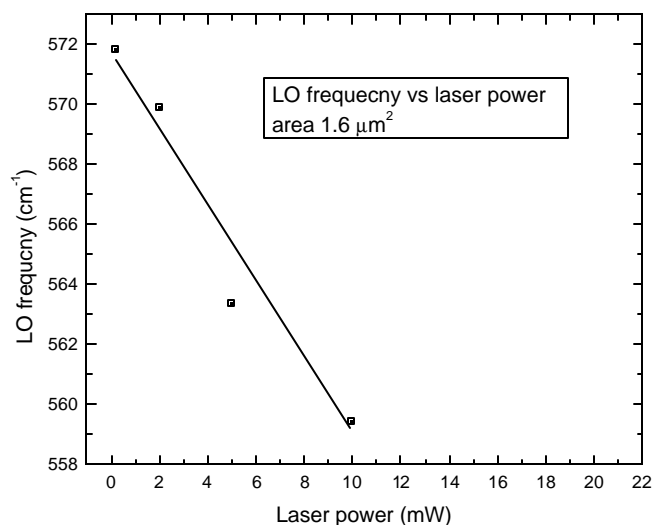


FIG. 4. LO phonon frequency shift in ZnO quantum dots as a function of laser power. Laser wavelength is 325 nm and laser spot area is $1.6 \mu\text{m}^2$.

The density of the nanocrystal powder is $0.3\text{--}0.45 \text{ g/cm}^3$, while for bulk ZnO is 5.6 g/cm^3 . This means that there is large amount of air between the QDs and therefore very small thermal conductivity of the nanocrystals. This explains the origin of such strong excitation laser heating effect in the Raman spectra of ZnO QDs. Taking into account the thermal expansion and anharmonic coupling effects, the LO phonon frequency can be calculated as

$$\begin{aligned}
w(T) = & \exp \left[-g \int_0^T \{ 2a_{\perp}(T') + a_{\parallel}(T') \} dT' \right] \times (w_0 - M_1 - M_2) + M_1 \left[1 + \frac{2}{e^{\hbar w_0 / 2 k_B T} - 1} \right] \\
& + M_2 \left[1 + \frac{3}{e^{\hbar w_0 / 3 k_B T} - 1} + \frac{3}{(e^{\hbar w_0 / 3 k_B T} - 1)^2} \right],
\end{aligned} \tag{1}$$

where the Grüneisen parameter g is taken from Ref. 9, the thermal expansion coefficients $a_{\perp}(T)$ and $a_{\parallel}(T)$ are taken from Ref. 10, and the anharmonicity parameters M_1 and M_2 are assumed to be equal to those of the $A_1(\text{LO})$ phonon of GaN [11]. By fitting of the experimental data shown in Fig. 4 with Eq. (1), the 14 cm^{-1} redshift is found corresponds to 700°C . Assuming LO peak shift in ZnO is proportional to UV laser power, using 20 mW laser power lead to 1400°C in the illuminated spot of the sample, which is evaporating temperature of powder nanocrystals.

CONCLUSION

We have identified the factors contributing to the phonon peak shifts in ZnO QDs. It has been established that there are three main mechanisms possible in this nanostructured material. Our experimental data shows that shift due to the optical phonon confinement and intrinsic defect in nanocrystals is few cm^{-1} while the laser-induced heating could result in a resonant Raman peak red shift as large as tens of cm^{-1} . The obtained results are important for interpretation of phonon spectrum from ZnO nanocrystals.

ACKNOWLEDGEMENT

This research has been supported through DARPA – SRC MARCO Center on Functional Engineered Nano Architectonics (FENA) and NSF Award to A.A.B

REFERENCES

1. V. A. Fonoberov and A. A. Balandin, *Appl. Phys. Lett.* **85**, 5971 (2004).
2. V. A. Fonoberov and A. A. Balandin, *Phys. Rev. B* **70**, 195410 (2004).
3. K. A. Alim, V. A. Fonoberov, and A. A. Balandin, *Appl. Phys. Lett.* **86**, 053103 (2005).
4. V. A. Fonoberov and A. A. Balandin, *Phys. Rev. B* **70**, 233205 (2004).
5. V. A. Fonoberov and A. A. Balandin, *J. Phys.: Condens. Matter* **17**, 1085 (2005).
6. V. A. Fonoberov and A. A. Balandin, *Phys. Status Solidi C* **1**, 2650 (2004).
7. N. Ashkenov, B. N. Mbenkum, C. Bundesmann, V. Riede, M. Lorenz, D. Spemann, E. M. Kaidashev, A. Kasic, M. Schubert, M. Grundmann, G. Wagner, H. Neumann, V. Darakchieva, H. Arwin, and B. Monemar, *J. Appl. Phys.* **93**, 126 (2003).
8. J. F. Scott, *Phys. Rev. B* **2**, 1209 (1970).
9. F. Decrempe, J. Pellicer-Porres, A. M. Saitta, J. C. Chervin, and A. Polian, *Phys. Rev. B* **65**, 092101 (2002).
10. H. Iwanaga, A. Kunishige, and S. Takeuchi, *J. Mat. Sci.* **35**, 2451 (2000).
11. W. S. Li, Z. X. Shen, Z. C. Feng, and S. J. Chua, *J. Appl. Phys.* **87**, 3332 (2000).